Journal of Food Composition and Analysis 153 (2026) 109143

Contents lists available at ScienceDirect

Journal of Food Composition and Analysis

journal homepage: www.elsevier.com/locate/jfca

Comparative multi-analytical characterization of lipid fractions from three cockroach species: *Blaptica dubia*, *Gromphadorhina portentosa*, and *Periplaneta lateralis*

Przemysław Łukasz Kowalczewski [a,1,*], Jan Jakub Kucharski [b,2], Ewa Ostrowska-Ligęza [c,3], Anna Grygier [b,4], Dominik Kmiecik [b,5], Wiktoria Kamińska [d,6], Aleksander Siger [e,7], Krzysztof Dwiecki [e,8], Przemysław Siejak [d,9], Dominika Radzikowska-Kujawska [f,10], Hanna Maria Baranowska [d,11]

[a] *Collegium Medicum, Andrzej Frycz Modrzewski Krakow University, Kraków, Poland*
[b] *Department of Food Technology of Plant Origin, Poznań University of Life Sciences, Poznań, Poland*
[c] *Department of Chemistry, Institute of Food Sciences, Warsaw University of Life Sciences, Warsaw, Poland*
[d] *Department of Physics and Biophysics, Poznań University of Life Sciences, Poznań, Poland*
[e] *Department of Biochemistry and Food Analysis, Poznań University of Life Sciences, Poznań, Poland*
[f] *Department of Agronomy, Poznań University of Life Sciences, Poznań, Poland*

ARTICLE INFO

Keywords:
Insect-derived oils
Lipid physicochemistry
Fatty acid profile
Oxidative stability
Tocopherols
Interfacial properties
Analytical characterization

ABSTRACT

This study presents a comprehensive, multi-analytical characterization of lipid fractions extracted from three cockroach species: *Blaptica dubia*, *Gromphadorhina portentosa*, and *Periplaneta lateralis*, with the aim of elucidating interspecies differences in fatty acid composition, molecular organization, and physicochemical behavior. Lipid fractions were analyzed using gas chromatography, Fourier transform infrared spectroscopy (FTIR), differential scanning calorimetry (DSC), low-field nuclear magnetic resonance (LF NMR) relaxometry, and Langmuir monolayer techniques. All oils were dominated by monounsaturated fatty acids, particularly oleic acid; however, marked differences were observed in the SFA/MUFA/PUFA balance, iodine values, thermal transitions, and interfacial properties. *B. dubia* oil exhibited the most balanced fatty acid profile and the most compact and viscoelastic monolayers, indicating a structurally stable lipid system. *G. portentosa* oil was characterized by the highest tocopherol content and enhanced oxidative resistance, whereas *P. lateralis* oil showed the highest degree of unsaturation accompanied by increased molecular mobility. The applied analytical techniques revealed distinct lipid structuring and stability patterns across species, demonstrating that cockroach-derived oils represent chemically and structurally diverse lipid matrices. These findings provide fundamental physicochemical

* Corresponding author.
E-mail addresses: pkowalczewski@uafm.edu.pl (P.Ł. Kowalczewski), jan.kucharski@up.poznan.pl (J.J. Kucharski), ewa_ostrowska_ligeza@sggw.edu.pl (E. Ostrowska-Ligęza), anna.grygier@up.poznan.pl (A. Grygier), dominik.kmiecik@up.poznan.pl (D. Kmiecik), wiktoria.kaminska@up.poznan.pl (W. Kamińska), aleksander.siger@up.poznan.pl (A. Siger), krzysztof.dwiecki@up.poznan.pl (K. Dwiecki), przemyslaw.siejak@up.poznan.pl (P. Siejak), dominika.radzikowska@up.poznan.pl (D. Radzikowska-Kujawska), hanna.baranowska@up.poznan.pl (H.M. Baranowska).
[1] 0000–0002-0153–4624
[2] 0009–0007-1351–8182
[3] 0000–0002-8387–8462
[4] 0000–0002-0529–3725
[5] 0000–0003-3708–2890
[6] 0009–0002-5935–6135
[7] 0000–0002-3681–153X
[8] 0000–0002-1438–1217
[9] 0000–0001-7519–6085
[10] 0000–0001-6989–1348
[11] 0000–0001-6597–0858

https://doi.org/10.1016/j.jfca.2026.109143
Received 11 August 2025; Received in revised form 21 March 2026; Accepted 6 April 2026
Available online 9 April 2026

insight into insect-derived lipids and establish a reference framework for future studies addressing technological performance, stabilization strategies, or regulatory assessment pathways.

1. Introduction

The global food sector is facing unprecedented challenges arising from the combined pressures of rapid population growth, limited natural resources, and the escalating consequences of climate change (Iqbal et al., 2025; Wijerathna-Yapa & Pathirana, 2022). Among critical nutrients, lipids represent not only a major source of energy but also contribute essential fatty acids and bioactive components crucial for human health (Kapoor et al., 2021). However, the sustainability of conventional animal-based lipids is increasingly questioned due to their environmental burden, competition for arable land, and vulnerability to climate-related disruptions. These constraints underline the necessity for identifying novel lipid sources that are environmentally sustainable, nutritionally adequate, and economically viable. In recent years, edible insects have emerged as a promising alternative, offering favorable nutritional profiles (Van Huis, 2013, Van Huis, 2020) and significantly lower environmental impacts compared to traditional livestock and, sometimes, oilseed crops as well (Moruzzo et al., 2021; Van Huis, 2022). While the lipid composition of certain insect groups - particularly coleopterans and orthopterans - has been extensively studied, research on cockroach species remains limited and fragmented. Yet, several cockroach species demonstrate advantageous biological traits, such as high reproductive efficiency, ease of mass rearing, and adaptability to diverse rearing substrates, which position them as potential candidates for sustainable lipid production (Idris, 2025; Siddiqui et al., 2024). Among these, *Blaptica dubia*, *Gromphadorhina portentosa*, and *Periplaneta lateralis* are of particular interest due to their broad availability in insect farming, high biomass yields, and preliminary reports indicating considerable lipid content.

Lipids are essential biomolecules that fulfill several vital physiological functions. In insects, they serve as an energy reservoir, a fundamental component of cellular membranes, and precursors to hormones and signaling molecules (Blomquist et al., 1991; Idris, 2025). Specifically in cockroaches, lipids play crucial roles in developmental transitions, thermoregulation, and metabolism, making them an important focus for studies related to entomophagy and insect-based bioproducts (Van Huis, 2013). The lipid profiles of cockroaches have been characterized by a predominance of monounsaturated and polyunsaturated fatty acids. Notably, oleic acid (C18:1n9c), linoleic acid (C18:2n6c), and α-linolenic acid (C18:3n3) have been identified as the principal components of cockroach lipid fractions (Rumpold & Schlüter, 2013).

From a nutritional standpoint, essential polyunsaturated fatty acids (PUFAs) such as linoleic and α-linolenic acids are critical to human health. These cannot be synthesized endogenously and must be acquired through diet to support neurological development, immune function, and inflammatory regulation (calder, 2015; Simopoulos, 2002). The presence of these fatty acids in cockroach species thus enhances their value as a sustainable source of dietary lipids. Nevertheless, alpha-linolenic acid levels tend to be relatively low in many cockroach species (often $<1.5\%$), suggesting that dietary enrichment or substrate manipulation during insect rearing could improve their nutritional profile (Perez-Santaescolastica et al., 2023).

Lipid composition in insects is influenced by a range of factors, including diet, environmental conditions, rearing substrates, and developmental stage (Barroso et al., 2014; Tzompa-Sosa et al., 2014). Furthermore, processing methods such as blanching, drying, or grinding can significantly affect lipid integrity and bioavailability (Lehmad et al., 2026; Sharma et al., 2022). Studies comparing raw and blanched samples of *Blaptica dubia* have shown reductions in total fat content and shifts in fatty acid profiles, highlighting the need to standardize processing techniques for optimal nutritional outcomes (Perez-Santaescolastica et al., 2023; Siddiqui et al., 2024). Despite growing interest in insect lipids, cockroach species remain relatively underrepresented in the literature compared to mealworms (*Tenebrio molitor*) or black soldier flies (*Hermetia illucens*). Yet cockroaches offer considerable advantages in terms of nutrient density, resilience, and ease of farming (Shelomi, 2015). Their protein and lipid profiles suggest broad applicability in the production of animal feed, human food supplements, and bio-based materials.

Nevertheless, comprehensive characterization of their lipid fractions remains largely unexplored. Existing studies often focus on total lipid content, providing insufficient information regarding the qualitative aspects that critically determine the functional and nutritional value of these lipids. It should be emphasized that, at the current stage, cockroach-derived oils are not authorized as food ingredients under the European Union Novel Food Regulation (EU) 2015/2283. Therefore, the present study is exploratory in nature and aims exclusively to characterize the physicochemical and nutritional features of these lipids. The oils analyzed in this work were not intended for human consumption, and any potential food application would require comprehensive toxicological evaluation and formal regulatory approval. Therefore, the aim of this research was a detailed and systematic evaluation encompassing fatty acid composition, oxidative stability, presence of bioactive minor compounds, and physicochemical properties to fully elucidate the potential applications of cockroach-derived lipids.

2. Materials and methods

2.1. Insects rearing and fat isolation

Three cockroach species were used in this study: the Madagascar hissing cockroach (*Gromphadorhina portentosa*, denotes as 'GP'), the Turkish cockroach (*Periplaneta lateralis*, 'PL'), and the Argentine cockroach (*Blaptica dubia*, 'BD'). All insects were reared in-house under controlled laboratory conditions until they reached full maturity. Only adult individuals were used for subsequent analyses, with no distinction made between sexes. The insects were maintained in plastic containers ($39 \times 39 \times 26$ cm) equipped with ventilation holes and secured with lids. Rearing conditions included a constant temperature of 26 °C, relative humidity maintained at 50–60%, and a photoperiod of 8 h light and 16 h darkness (8 L:16D). Throughout the rearing period, insects were fed *ad libitum* with a standardized diet composed of 18% crude protein, 5% crude fat, 4.5% crude fiber, 12% ash. Water was also provided without restriction to ensure optimal hydration. Upon reaching adulthood, the insects were subjected to a 24-hour starvation period to allow for gut clearance. They were then frozen at −82 °C for 12 h and lyophilized for 24 h under vacuum (0.1 mbar) using a freeze dryer (Alpha 2–4 LD_{plus}, Martin Christ, Osterode am Harz, Germany). The lyophilized insects were initially ground using a laboratory mill with temperature control (IKA, Staufen, Germany) to prevent thermal degradation of sensitive components. The final insect flour was vacuum-sealed and stored at −20 °C until further use.

Total lipids were extracted from the insect powders using the Folch method (Folch et al., 1957). This classical extraction procedure is based on the partitioning of lipids into a chloroform-methanol mixture (2:1, v/v), which effectively solubilizes neutral and polar lipids from complex biological matrices. The extraction was carried out over 24 h at room temperature, under continuous agitation, to ensure maximum lipid

recovery. After extraction, the organic phase was separated, filtered, and evaporated under reduced pressure. The resulting lipid fractions were weighed and stored at −72 °C until further analysis. All samples were prepared exclusively for analytical purposes and were not intended for any food-related use.

2.2. Color analysis

The color of the extracted oils was measured in the CIE L*a*b* color space using a Spectro Pen LMV 169 (Hach Lange GmbH, Germany). The lightness parameter (L*) was recorded, along with chromatic coordinates a* and b*, representing red (+)/green (–) and yellow (+)/blue (–) saturation levels, respectively. Measurements were performed under standardized conditions following the manufacturer's guidelines.

2.3. Fatty acid composition

The fatty acid composition was determined in accordance with the AOCS Official Method Ce 1h-05 (AOCS, 2009b). Fat samples were dissolved in *n*-hexane and transesterified with 0.1 M sodium methylate. After transesterification process the hexane layer was transferred to vials for analyses. The resulting fatty acid methyl esters (FAMEs) were separated using an Agilent 8890 GC System (Agilent Technologies, Santa Clara, CA, USA) equipped with an SLB-IL111 capillary column (100 m × 0.25 mm i.d., 0.20 μm) (Supelco, Bellefonte, PA, USA) and detected with a flame ionization detector (FID). The oven temperature was programmed to increase from 150 °C to 200 °C at a rate of 1.5 °C/min. The injector and detector were maintained at 250 °C, operating with a split ratio of 1:10. The carrier gas was a hydrogen with a constant flow rate of 1 mL/min. Fatty acid methyl esters (FAMEs) were identified and quantified using highly pure reference standards (Supelco 37 Component FAME Mix, Merck, Darmstadt, Germany). The identification was confirmed by matching retention times with the reference standards under strictly controlled GC conditions, in full compliance with the validated AOCS Official Method Ce 1h-05 parameters.

2.4. Calculated iodine value (CIV)

The calculated iodine value (CIV) was conducted according to the AOCS Official Method Cd 1c-85 (AOCS, 2009a) and calculated from fatty acid composition. The method of calculation is based on the percentage of hexadecenoic acid, octadecenoic acid, octadecadienoic acid, octadecatrienoic acid, eicosanoid acid, and docosenoic acid.

2.5. Nutritional quality indicators of oils

2.5.1. Polyunsaturated fatty acid/saturated fatty acid (PUFA/SFA) ratio

The PUFA/SFA ratio is an index normally used to inform about the impact of diet on cardiovascular health (Chen & Liu, 2020). The underlying assumption is that polyunsaturated fatty acids (PUFAs) help reduce serum LDL cholesterol, whereas saturated fatty acids (SFAs) tend to increase it. Therefore, a higher PUFA/SFA ratio is generally considered indicative of a more favorable dietary lipid profile. The PUFA/SFA index of analyzed oils was also calculated.

2.5.2. Index of atherogenicity (IA)

The IA index shows the reciprocal relationship between the sum of SFA and the sum of unsaturated fatty acids (UFA) in foods. However, only C12:0, C14:0, and C16:0 acids are considered proatherogenic. Unsaturated fatty acids are considered antiatherogenic because they inhibit atherosclerotic plaque deposition and reduce phospholipid and cholesterol levels (Ulbricht & Southgate, 1991). The IA index was calculated based on the formula 1:

$$IA = \frac{C12:0 + (4 \times C14:0) + C16:0}{\Sigma UFA} \quad (1)$$

2.5.3. Index of thrombogenicity (IT)

The IT index characterizes the thrombogenic potential of fatty acid, indicating the tendency to form clots in blood vessels. The index determines the relationship between prothrombogenic (SFA) and antithrombogenic fatty acids (MUFA, n3, and n6 PUFA) (Ulbricht & Southgate, 1991). The IT index was calculated based on the formula 2:

$$IT = \frac{C14:0 + C16:0 + C18:0}{(0.5 \times \Sigma MUFA) + (0.5 \times \Sigma n6PUFA) + (3 \times \Sigma n3PUFA) + (\Sigma n3PUFA/\Sigma n6PUFA)} \quad (2)$$

2.5.4. Hypocholesterolemic/hypercholesterolemic (HH) ratio

The HH ratio illustrates the relationship between hypocholesterolemic and hypercholesterolemic fatty acids. Mainly, it is the relationship between sum of oleic acid (C 18:1) and polyunsaturated fatty acids (hypocholesterolemic part), and saturated fatty acids from C 12:0 to C 16:0 (hypercholesterolemic part) (Chen & Liu, 2020). The HH ratio index was calculated based on the formula 3:

$$HH = \frac{cis - C18:1 + \Sigma PUFA}{C12:0 + C14:0 + C16:0} \quad (3)$$

2.6. Sterols content measurement

For phytosterols determination the AOCS Official Method Ch 6–91 (AOCS, 2009c) with modification (Rudzińska et al., 2025) was used. For saponification 1 M KOH in methanol were added to the samples. The samples were heated 1 h at 40 °C. After 18 h at room temperature the reaction was stopped by adding water. Phytosterols were extracted using a mixture of hexan:methyl tert-butyl ether (MTBE) (1:1, v:v). The solvent was evaporated by nitrogen gas. The samples were silylated with *N*,*O*-Bis(trimethylsilyl)trifluoroacetamide (BSTFA) + 1% trimethylsilyl chloride (TMCS) (Supelco, Saint Louis, USA). A gas chromatograph 7820 A (Agilent Technologies, California, USA) with flame ionization detector (FID) was used for separation. The separation was performed on DB-35MS (25 m × 0.20 mm; 0.33 μm; J&W Scientific, Folsom, USA) capillary column. The oven temperature was 100 °C for 5 min, then increased to 250 °C at 25 °C/min, held for 1 min, then raised to 290 °C at 3 °C/min and held for 20 min. The temperature of injector and detector were set at 300 °C. The flow rate of hydrogen was 1.5 mL/min. Phytosterols were reliably identified by matching their retention times with highly pure reference standards. Quantification was performed using 5α-cholestane as an internal standard to ensure high accuracy and precision of the analytical procedure.

2.7. Tocopherols content analysis

Tocpopherols contents were assayed and calculated according to (Siger et al., 2014). Oil (200 mg) was dissolved in *n*-hexane, made up to 10 mL, and transferred to vials for analyses. Tocopherols were qualitatively and quantitatively identified using a Waters HPLC system (Waters,

Milford, MA) consisting of a pump (Waters 600), a fluorimetric detector (Waters 474), a photodiode array detector (Waters 2998 PDA), which was used to identify tocochromanols based on their UV–Vis spectra, an autosampler (Waters 2707), a column oven (Waters Jetstream 2 Plus), and a LiChrosorb Si 60 column (250 × 4.6 mm, 5 μm) by Merck (Darmstadt, Germany). The mobile phase was a mixture of *n*-hexane with 1,4-dioxane (96:4 v/v). The flow rates were 1.0 mL/min. To detect the fluorescence of tocopherols, the excitation wavelength was set at λ = 295 nm and the emission wavelength at λ = 330 nm. Standards of α-, β-, γ- and δ-tocopherols (> 95% of purity) were purchased from Merck (Darmstadt, Germany). Compound identification was performed by comparison of both retention times and UV–Vis spectra with those of authentic external standards. The vitamin E content was calculated as the sum of the biological activities of individual tocopherol and tocotrienol homologues, expressed in α-tocopherol equivalents (α-TE), according to the following formula 4 (Eitenmiller & Lee, 2004):

α-TE (mg) = 1.0 × mg α-T + 0.5 × mg β-T + 0.1 × mg γ-T + 0.03 × mg δ-T + 0.5 × mg α-T3 + 0.05 × mg β-T3 + 0.01 × mg γ-T3 (Eq. 4)

Full validation parameters of the applied HPLC method, including linearity, limits of detection and quantification (LOD and LOQ), precision, and accuracy, were previously established and reported in our earlier study (Siger et al., 2014)

2.8. Water content

Water content in oils was measured using the Karl-Fischer method in accordance with ISO 8534 (ISO, 2008) method.

2.9. Melting characteristics measured by differential scanning calorimetry (DSC)

DSC measurements of melting characteristics of oils were carried out with a TA DSC Q200 (TA Instruments Corporate, New Castle, DE, USA). Calibration was done with pure indium of high purity. Inset oil samples of 3–4 mg were placed into aluminum pans with a lid and were hermetically sealed. An empty sealed aluminum pan was used as a reference, and the experiments were performed under a nitrogen atmosphere at normal pressure. Melted samples were heated to 80 °C and held for 10 min, in order to melt all the crystals and to erase the thermal memory. The samples were then cooled to −80 °C at 10 °C/min and maintained at −80 °C for 30 min. Then the melting profiles were obtained by heating the samples to 80 °C at a heating rate of 15 °C/min (Wirkowska et al., 2012).

2.10. Fourier transform infrared spectroscopy (FTIR) analysis

Infrared spectra were gathered using a Perkin Elmer spectrophotometer (Waltham, MA, USA), which was equipped with an ATR device featuring a diamond as its internal reflection element in the spectral range of 4000 - 400 cm^{-1} (Kamińska et al., 2023).

2.11. LF NMR spectrometry

The Low-Field Nuclear Magnetic Resonance (LF NMR) technique was applied to analyzed proton dynamics in oils (Cichocki et al., 2023). All measurements were performed at controlled temperature 20.0 ± 0.5 °C. The spin–lattice (T_1) and spin–spin (T_2) relaxation times were measured by using pulse NMR spectrometer PS15T (Ellab, Poznań, Poland) operating at 15 MHz. The inversion-recovery (π–t–(π/2)) pulse sequence was applied to T_1 relaxation times measurements. Distances (t) between RF pulses were changed within the range of 0.5–200 ms and it was different for different samples. In all cases, the 13 s repetition time was used. The 32 FID signals and 110 points of each FID signal were collected.

Measurements of T_2 spin-spin relaxation times were taken using the pulse train of Carr-Purcell-Meiboom-Gill spin echoes ($(\pi/2)$-t-$(\pi)_n$) (Carr & Purcell, 1954; Meiboom & Gill, 1958). The distance t between the RF pulses was 2 ms and the repetition time was 15 s. The number of spin echoes (n) was 100.

Calculations of spin-lattice relaxation time values were performed with CracSpin software (Jagiellonian University, Cracow, Poland) (Węglarz & Harańczyk, 2000) using a "spin grouping" approach. The precision of the relaxation parameters was determined, and the standard deviations were calculated. The recovery of the magnetization is described by the Eq. 5:

$$M_z(t) = M_0\left[1 - 2e^{\frac{-t}{T_1}}\right] \quad (5)$$

where: $M_z(t)$ is the actual magnetization value, and M_0 is the equilibrium magnetization values.

The calculation of spin-spin relaxation time values was based on adjustment of echo amplitude values to Eq. 6:

$$M_{x,y}(t) = M_0 e^{\frac{-t}{T_2}} \quad (6)$$

where: $M_{x,y}$ (t) is the echo amplitude; M_0 is the equilibrium amplitude.

The calculations were performed with TableCurve2D® v5.01.02 software using a nonlinear least-squares algorithm. The standard deviation was used to determine the accuracy of both relaxation parameters.

2.12. Formation of monolayers at the air-water interface

Monolayers composed of selected oils were studied using a Langmuir trough (model KN 2002, KSV NIMA, Helsinki, Finland), which featured two hydrophilic barriers moving symmetrically. The trough, constructed from Teflon, offered a working surface of 273 cm^2 and held a subphase volume of 176 mL. Before conducting experiments, it was meticulously washed with methanol and chloroform (99.8% purity, POCH, Lublin, Poland). Ultrapure, deionized water with a resistivity of 18.2 MΩ·cm, sourced from a Milli-Q system, served as the subphase. The water surface was cleaned using an external aspirator pump until surface pressure fluctuations following full barrier movement were below 0.1 mN/m.

A measured quantity of the oil sample was applied drop by drop onto the cleaned water surface using a high-precision microsyringe (Hamilton, Reno, NV, USA). After a 10-minute wait to allow the chloroform to evaporate, the monolayer was compressed at a constant speed of 5 mm/min. Surface pressure (π) was continuously monitored in relation to the average molecular area (A), using a porous platinum Wilhelmy plate suspended from an electronic balance with 0.01 mN/m precision. To ensure data reliability, each surface pressure–area (π–A) isotherm was obtained at least three times, with a reproducibility error of no more than ±0.02 cm^2. These π–A isotherms described how surface pressure changes as the area per molecule varies. Surface pressure is defined as the difference between the surface tension of the pure subphase (σ_o) and that of the monolayer-covered surface (σ), expressed as (Kamińska et al., 2023):

$$\pi = \sigma_o - \sigma \quad (7)$$

Alterations in surface pressure reflect changes in molecular spacing, which in turn influence the physical properties of the monolayer, such as its fluidity and elasticity. The compressibility modulus (C_S^{-1}), which indicates the elastic nature of the monolayer, is calculated using the formula 8 (Piotrowska-Kirschling et al., 2018):

$$C_s^{-1} = -A\left[\frac{d\pi}{dA}\right]_T \quad (8)$$

Where: A represents the molecular area and π is the measured surface pressure.

Table 1
Color parameters of obtained oils.

Sample	L*	a*	b*
GP	42.66 ± 1.44^{c}	6.57 ± 0.88^{b}	-3.28 ± 0.45^{b}
BD	45.70 ± 1.05^{b}	7.06 ± 0.75^{b}	-2.13 ± 0.32^{b}
PL	53.53 ± 2.91^{a}	12.21 ± 0.91^{a}	17.49 ± 0.79^{a}

Values marked with the same lowercase letter in columns do not differ significantly $p > 0.05$. GP - *Gromphadorhina portentosa,* PL - *Periplaneta lateralis* BD - *Blaptica dubia*

2.13. Oscillatory barrier experiment

The dilational viscoelastic properties of the Langmuir monolayers were assessed using the oscillating barrier technique. Following compression to a predetermined surface pressure, the films were allowed to equilibrate for 20 min. Subsequently, the barriers were subjected to periodic motion at a frequency of 0.1 Hz, generating sinusoidal area changes with a relative amplitude of 5%.

The resulting surface pressure variations induced by the periodic compression–expansion cycles were recorded. Each experiment included a minimum of five oscillation cycles, with 60-second intervals between successive cycles. The method allowed determination of the elastic and viscous components of the monolayer's response to dynamic area perturbation. Dilational interfacial rheology may be investigated using different modes of deformation, including transient or oscillatory (harmonic) changes in surface area. The expression describing dilational viscoelasticity, denoted as ε, is provided by the Eq. 9 (Luviano et al., 2019; Noskov & Bykov, 2018):

$$E = -A\left[\frac{d\pi}{dA}\right] \quad (9)$$

2.14. Statistical analysis

All the results were repeated in triplicate, unless stated otherwise, then the mean values were reported from them along with the corresponding standard deviations (SD). The tables show the statistically significant differences, which were evaluated by one-way ANOVA Tukey's test at a significance level of $p \leq 0.05$ using Statistica v13.3 (Dell Software Inc., USA).

3. Results and discussion

3.1. Color analysis

The color parameters of the oils showed pronounced, statistically significant differences among species (Table 1). The lightness (L*) ranged from 42.66 in GP to 53.53 in PL, indicating that PL oil was visibly the brightest, while GP oil appeared the darkest. The chromatic coordinates further emphasized species-specific variation. GP and BD oils were characterized by negative b* values (–3.28 and –2.13, respectively), indicating a slightly bluish–green hue, whereas PL oil exhibited a strongly positive b* value (17.49), demonstrating a clear yellow tone. The a* parameter also differed substantially, with PL showing the highest positive value (12.21), reflecting a noticeable reddish tint, while GP and BD remained moderately red (6.57 and 7.06, respectively).

These differences in color are easily perceptible to the naked eye and correspond directly to the visual appearance of the samples shown in Fig. 1, where PL oil presents an intense yellow-amber coloration, BD a pale golden color, and GP a darker, brownish tone. Such variation may be associated with species-dependent differences in lipid composition, including tocopherol concentrations, degree of unsaturation, and potential presence of minor pigments or oxidation products. The particularly high b* and a* values in PL oil suggest a greater abundance of chromophoric compounds or increased susceptibility to oxidation-related color changes, consistent with its elevated PUFA content.

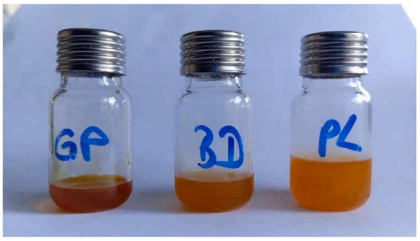

Fig. 1. Photograph of obtained oils. GP - *Gromphadorhina portentosa,* PL - *Periplaneta lateralis* BD - *Blaptica dubia.*

Table 2
Fatty acid compositions (%) and calculated Iodine Value of analyzed oils.

Fatty acid	GP	BD	PL
C 12:0	Nd	0.14 ± 0.01a	0.09 ± 0.00^{b}
C 14:0	0.53 ± 0.01^{b}	1.05 ± 0.01a	1.13 ± 0.01^{a}
C 16:0	19.01 ± 0.01^{b}	16.27 ± 0.01c	20.43 ± 0.02^{a}
C 16:1	5.80 ± 0.01^{b}	8.02 ± 0.02^{a}	2.92 ± 0.01^{c}
C 18:0	6.06 ± 0.01^{a}	3.52 ± 0.01^{b}	3.52 ± 0.15^{b}
C 18:1	54.45 ± 0.08^{b}	59.45 ± 0.01^{a}	54.56 ± 0.07^{b}
C 18:2	13.59 ± 0.08^{b}	10.94 ± 0.03^{c}	16.38 ± 0.02^{a}
C 18:3	0.56 ± 0.01^{b}	0.61 ± 0.01^{b}	0.97 ± 0.08^{a}
∑SFA	25.60	20.98	25.17
∑MUFA	60.25	67.47	57.57
∑PUFA	14.15	11.55	17.35
CIV	77.34 ± 0.05^{b}	79.29 ± 0.03^{a}	80.60 ± 0.31^{a}

Values marked with the same lowercase letter in rows do not differ significantly $p > 0.05$. Nd – not detected, CIV – calculated Iodine Value, GP - *Gromphadorhina portentosa,* PL - *Periplaneta lateralis* BD - *Blaptica dubia*

3.2. Fatty acid composition

The fatty acid profiles of oils extracted from *Gromphadorhina portentosa* (GP), *Blaptica dubia* (BD), and *Periplaneta lateralis* (PL) are summarized in Table 2. The oils were predominantly composed of monounsaturated fatty acids (MUFA), with oleic acid (C18:1) being the major component in all species. BD oil contained the highest proportion of C18:1 (59.45%), followed by PL (54.56%) and GP (54.45%), with statistically significant differences ($p < 0.05$) observed between BD and the other two species. Palmitic acid (C16:0) was the predominant saturated fatty acid (SFA), with the highest level detected in PL oil (20.43%), significantly higher than in GP (19.01%) and BD (16.27%). Stearic acid (C18:0) was more abundant in GP (6.06%) than in BD and PL (both 3.52%). These differences indicate that GP oil has the highest overall SFA share among the three, which may affect its oxidative stability and thermal behavior (Gao & Birch, 2016; Hoshina et al., 2004). BD oil exhibited the highest share of palmitoleic acid (C16:1; 8.02%), a

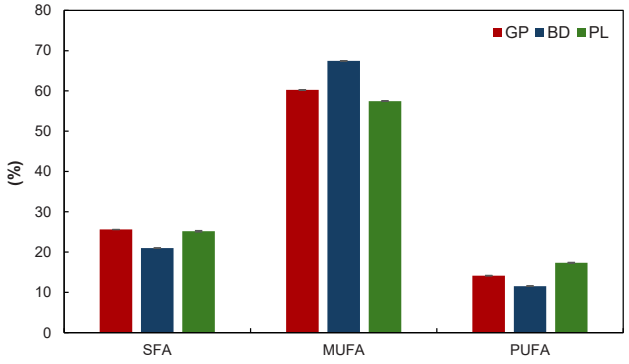

Fig. 2. Sum of saturated (SFA), monounsaturated (MUFA) and polyunsaturated fatty acid (PUFA) in analyzed oils. GP - *Gromphadorhina portentosa,* PL - *Periplaneta lateralis,* BD - *Blaptica dubia.*

MUFA associated with health-promoting effects, while PL showed the lowest level (2.92%). The presence of lauric (C12:0) and myristic (C14:0) acids was minor but significantly different between the oils, with BD and PL containing higher levels than GP. Polyunsaturated fatty acids (PUFA) were primarily represented by linoleic acid (C18:2) and α-linolenic acid (C18:3). PL oil had the highest linoleic acid share (16.38%), followed by GP (13.59%) and BD (10.94%). The level of α-linolenic acid was also highest in PL (0.97%) and lowest in GP (0.56%). As expected, the calculated iodine value (CIV), which reflects the degree of unsaturation, was highest for PL (80.60), followed by BD (79.29) and GP (77.34), with BD and PL not differing significantly ($p > 0.05$).

These results highlight distinct lipidomic signatures among the cockroach species (Fig. 2). BD oil is characterized by high oleic and palmitoleic acid contents, suggesting good oxidative stability and health-oriented lipid quality (Kmiecik et al., 2022). GP oil, richer in saturated fatty acids, may offer better structural functionality in solid or semi-solid fat applications. PL oil, due to its elevated PUFA levels, may present enhanced nutritional value, but at the cost of potentially reduced oxidative stability (Nogueira et al., 2019). The fatty acid distribution observed in the present study is consistent with previous reports on cockroach species and other edible insects, where high proportions of MUFA and PUFA and relatively low SFA levels are typically described. Similar dominance of oleic and linoleic acids has been reported for *Blaptica dubia* and *Periplaneta americana* oils as well as for cricket, mealworm, and locust lipids, indicating that such profiles may be characteristic for many hemimetabolous and holometabolous insect taxa (Kolobe et al., 2023; Palupi et al., 2025; Perez-Santaescolastica et al., 2023).

3.3. Nutritional quality indicators

The nutritional quality of the extracted oils was evaluated based on four commonly used indices (Table 3). The PUFA/SFA ratio, an indicator of the potential lipid-lowering effect and cardiovascular benefits of dietary fats (Petersen et al., 2024), was significantly higher in PL oil (0.69 ± 0.01) compared to GP and BD oils (both 0.55 ± 0.00; $p < 0.05$). This suggests a more favorable unsaturated fatty acid profile in PL oil, consistent with its elevated linoleic acid content. The IA, which reflects the potential to promote lipid deposition in arteries (Khalili Tilami & Kouřimská, 2022), ranged from 0.26 in BD to 0.34 in PL oils. Although the values were relatively low for all samples, PL oil exhibited the highest IA, which may be attributed to its higher proportion of palmitic acid (C16:0). Similarly, the IT, which estimates the likelihood of thrombus formation (Khalili Tilami & Kouřimská, 2022), was lowest in BD oil (0.51), followed by PL (0.63) and GP (0.66) oils. These differences correspond to the relative proportions of MUFA and PUFA, particularly oleic and linoleic acids, known for their anti-thrombogenic properties. The HH ratio provides an overall measure of the cholesterol-modulating effect of dietary fats (Chen & Liu, 2020). BD oil displayed the most favorable HH ratio (4.07 ± 0.01), while GP and PL showed slightly lower values (3.51 ± 0.00 and 3.32 ± 0.01, respectively). The higher HH ratio in BD is mainly attributed to its elevated content of oleic acid and comparatively lower levels of C14:0 and C16:0. Taken together, the data suggest that while all three oils possess nutritionally advantageous profiles, BD oil demonstrates the most favorable overall health-related lipid indices, particularly in terms of hypocholesterolemic potential and anti-thrombogenicity. These characteristics may enhance its applicability as a functional lipid ingredient.

Table 3
Nutritional indices used to assess the nutritional quality of oils.

Sample	PUFA/SFA	IA	IT	HH
GP	0.55 ± 0.00^{b}	0.28 ± 0.00^{b}	0.66 ± 0.01^{a}	3.51 ± 0.00^{b}
BD	0.55 ± 0.00^{b}	0.26 ± 0.01^{b}	0.51 ± 0.00^{c}	4.07 ± 0.01^{a}
PL	0.69 ± 0.01^{a}	0.34 ± 0.00^{a}	0.63 ± 0.01^{b}	3.32 ± 0.01^{c}

Values marked with the same lowercase letter in columns do not differ significantly $p > 0.05$. IA - index of atherogenicity; IT - index of thrombogenicity; HH - hypocholesterolemic/hypercholesterolemic ratio. GP - *Gromphadorhina portentosa,* PL - *Periplaneta lateralis,* BD - *Blaptica dubia.*

Table 4
Sterol contents in analyzed oils (mg/g).

Sample	Cholesterol	Campesterol	β-Sitosterol
GP	4.41 ± 0.09^{a}	Nd	0.31 ± 0.05^{b}
BD	3.15 ± 0.01^{b}	0.78 ± 0.00	0.56 ± 0.05^{a}
PL	2.44 ± 0.27^{c}	Nd	0.17 ± 0.03^{c}

Values marked with the same lowercase letter in columns do not differ significantly $p > 0.05$. Nd – not detected, GP - *Gromphadorhina portentosa,* PL - *Periplaneta lateralis* BD - *Blaptica dubia*

3.4. Sterols

The sterol profiles of the insect-derived oils are presented in Table 4. Cholesterol was the predominant sterol in all samples, with significant differences in its concentration among species ($p < 0.05$). The highest cholesterol content was found in GP oil (4.41 ± 0.09 mg/g), followed by BD (3.15 ± 0.01 mg/g), and the lowest in PL (2.44 ± 0.27 mg/g). These findings are in agreement with previous reports indicating cholesterol as the major sterol in most insect lipid fractions (Mudalungu et al., 2023a), reflecting the animal origin of these fats. β-Sitosterol, a plant-derived phytosterol often associated with cholesterol-lowering properties (Durrani et al., 2024), was also detected in all samples but at markedly lower concentrations. The highest β-sitosterol level was observed in BD oil (0.56 ± 0.05 mg/g), which was significantly higher than in GP (0.31 ± 0.05 mg/g) and PL (0.17 ± 0.03 mg/g). The presence of β-sitosterol in insect oils may be linked to dietary intake or metabolic transformation of plant-derived sterols consumed during rearing (Mudalungu et al., 2023a). Interestingly, campesterol was exclusively detected in BD oil (0.78 ± 0.00 mg/g), whereas it was not found in GP or PL samples. The detection of this phytosterol in BD oil could suggest differences in the metabolic assimilation of dietary components. The sterol content and composition varied significantly among the three species, with *Blaptica dubia* oil distinguished by the presence of campesterol and the highest β-sitosterol level. These features may enhance its potential nutritional value due to the combined presence of both animal- and plant-derived sterols. The sterol composition observed in the analyzed oils aligns with previous studies showing cholesterol as the predominant sterol in insect-derived lipids, accompanied by smaller amounts of campesterol and β-sitosterol. Comparable sterol patterns have been found in other edible insect oils, including those of crickets, mealworms, and cockroaches, suggesting a conserved sterol biosynthesis pathway across species (Jing & Behmer, 2020; Mudalungu et al., 2023b).

3.5. Tocopherols

The qualitative and quantitative profiles of tocopherols in oils are presented in Table 5. α-tocopherol was the dominant isomer in all samples, with levels ranging from 2.03 to 5.98 mg/100 g. GP oil exhibited the highest total tocopherol content (6.45 ± 0.01 mg/100 g), primarily composed of α-tocopherol (5.98 ± 0.00 mg/100 g), along with small amounts of β- and γ-tocopherol. BD oil contained only α-tocopherol (3.15 ± 0.01 mg/100 g), whereas PL oil contained all three detected isomers, although at lower overall levels (2.38 ± 0.01 mg/100 g total tocopherols).

The calculated vitamin E activity, expressed as α-tocopherol equivalents, followed a similar trend: GP > BD > PL, with values of 6.17, 3.15, and 2.16 mg/100 g, respectively. This is consistent with the known biological potency of α-tocopherol relative to other isomers.

Table 5
Tocopherol contents in analyzed oils (mg/100 g of oil).

Sample	α-Tocopherol	β-Tocopherol	γ-Tocopherol	Total tocopherols	Vitamin E
GP	5.98 ± 0.02a	0.37 ± 0.02[a]	0.10 ± 0.01[a]	6.45 ± 0.03[a]	6.17 ± 0.03[a]
BD	3.15 ± 0.01b	Nd	Nd	3.15 ± 0.01[b]	3.15 ± 0.01[b]
PL	2.03 ± 0.01c	0.26 ± 0.01[b]	0.10 ± 0.01[a]	2.38 ± 0.01[c]	2.16 ± 0.00[c]

Values marked with the same lowercase letter in columns do not differ significantly $p > 0.05$. Nd – not detected, GP - *Gromphadorhina portentosa,* PL - *Periplaneta lateralis* BD - *Blaptica dubia*

Tocopherols are lipid-soluble antioxidants with both nutritional and functional significance. Their presence not only contributes to vitamin E activity in the human diet but also enhances the oxidative stability of oils by scavenging lipid radicals and inhibiting lipid peroxidation (Mishra et al., 2021). The relatively high tocopherol content in GP oil, particularly of α-tocopherol, suggests improved resistance to oxidative degradation, which is advantageous for applications in food systems requiring prolonged shelf-life. The absence of β- and γ-tocopherol in BD oil and the overall lower tocopherol content in PL oil may limit their oxidative stability (Kamal-Eldin, 2006), particularly in the case of PL, which also exhibits a high PUFA content. Since tocopherols are typically derived from dietary sources in insects, the observed differences may reflect variations in feed composition or metabolic processing among the species (Sabolová et al., 2016; Yap et al., 2023). Our results indicate that oils from *G. portentosa* may offer superior oxidative stability and nutritional value with respect to vitamin E, while *B. dubia* oil provides a moderate level of antioxidant protection. *P. lateralis* oil, despite its favorable PUFA profile, may require additional stabilization when used in food formulations.

3.6. Water content

Water content is a critical parameter influencing the oxidative stability, shelf life, and processing behavior of edible oils (Budilarto & Kamal-Eldin, 2015). It is important to emphasize that all three oils were extracted using the same Folch protocol, which ensures methodical consistency across samples. In this method, one of the final steps prior to solvent evaporation involves drying the extract; however, trace amounts of water may remain, as small quantities of bound or naturally occurring moisture are typical constituents of oils and fats. Therefore, the observed differences likely reflect species-specific lipid microstructures rather than procedural variation. The results of Karl Fischer titration (Fig. 3) revealed significant differences among the oils extracted from GP, BD, and PL. GP oil exhibited the highest moisture content, significantly greater than that observed in BD and PL oils. Elevated water content in GP oil may be attributed to species-specific differences in tissue hydration or extraction efficiency, as well as possible variations in the microstructure or emulsion-forming capacity of the lipid matrix (Dos Santos et al., 2025). This relatively high moisture level could negatively affect oil stability by promoting hydrolytic rancidity and increasing susceptibility to microbial growth, particularly if the oil is stored under suboptimal conditions (Martín-Torres et al., 2022; Oh et al., 2015). The lowest water content was observed in BD oil. This result, in combination with its moderate degree of unsaturation and relatively high tocopherol concentration, suggests enhanced oxidative stability and prolonged shelf-life (Siger & Michalak, 2016; Ying et al., 2018). PL oil, despite its higher PUFA content, displayed an intermediate water level, which could partially compromise its oxidative stability unless antioxidants or appropriate packaging technologies are applied. As water content alone cannot be considered a reliable indicator of oxidative stability, the present study applied advanced analytical techniques to more accurately characterize the oils' functional behavior. Differential scanning calorimetry (DSC) provided insight into triacylglycerol melting transitions and thermal stability, while LF NMR relaxometry enabled assessment of molecular mobility and proton dynamics. These complementary methods allowed for a deeper mechanistic interpretation beyond the moisture data alone.

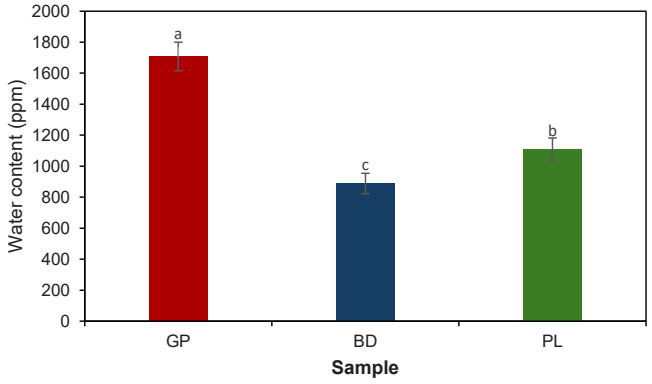

Fig. 3. Water content results measured by Karl-Fischer titration method. GP - *Gromphadorhina portentosa*, PL - *Periplaneta lateralis*, BD - *Blaptica dubia*.

3.7. DSC study

Thermal properties of the lipid fractions were assessed using differential scanning calorimetry (DSC), and the results are presented in Fig. 4. Each sample exhibited a distinct melting profile, characterized by multiple endothermic transitions, indicative of a heterogeneous triacylglycerol (TAG) composition. All lipids displayed an initial minor endothermic peak in the ultra-low temperature region (approximately −72 °C), which may be attributed to baseline noise or equipment inertia. In the DSC thermogram of the BD lipid, a single pronounced endothermic event was observed, with a phase transition at −13.04 °C, suggesting the presence of low-melting TAG fractions rich in polyunsaturated fatty acids (PUFAs). BD lipid exhibited the highest combined content of PUFAs and monounsaturated fatty acids (MUFAs), reaching 79.02% (Table 2), which may explain the low transition temperature. The TAG composition likely influenced the maximum peak

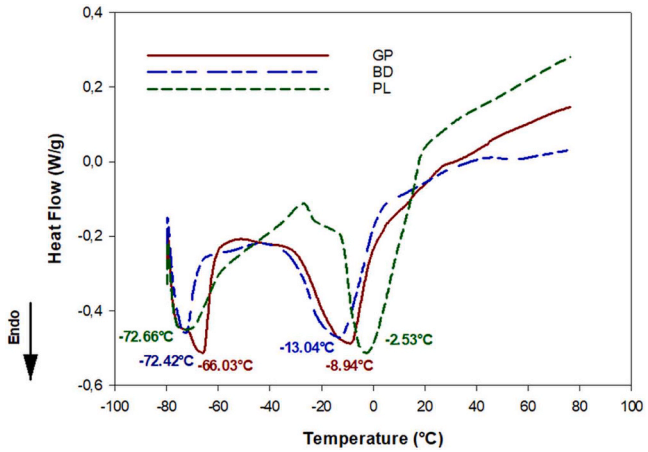

Fig. 4. DSC melting characteristics of insect oils. GP - *Gromphadorhina portentosa*, PL - *Periplaneta lateralis*, BD - *Blaptica dubia*.

temperature of the BD lipid. For comparison, Siejak et al. (2025) reported endothermic events at −20 and −17 °C in elderberry seed oil, similarly associated with high PUFA levels.

Although PL lipid contained the highest proportion of PUFAs among the tested samples, its maximum melting peak was observed at −2.53 °C (Fig. 3), indicating differences in TAG structure that modulate melting behavior. The melting curve of the GP lipid showed a maximum endothermic peak at −8.94 °C, also reflecting the presence of low-melting TAG fractions. Notably, the GP and PL lipids exhibited the lowest peak temperatures overall (Fig. 3). While PUFA and MUFA contents were comparable between GP and PL lipids (Table 2), the presence of higher amounts of saturated fatty acids may have contributed to differences in TAG composition and, consequently, to the melting behavior. The specific TAG structure appears to significantly influence both the shape and temperature of the observed melting transitions. Similar observations were reported by Górska et al. (2023), who characterized the melting profiles of cranberry, blackcurrant, and strawberry seed oils, with endothermic peaks ranging from −40.23 °C to −20.87 °C. These findings support the hypothesis that the diversity in TAG molecular species and high unsaturation levels contribute to the wide range of melting behaviors. Comparable conclusions were drawn by Wirkowska-Wojdyła et al. (2022) in studies on amaranth and quinoa oils.

Among all tested samples, the PL lipid exhibited the highest enthalpy of fusion (ΔH), with a value of 64.31 ± 1.15 J/g, and its melting curve was characterized by the broadest peak, suggesting the presence of a wide range of TAG species. In contrast, the BD and GP lipids demonstrated lower enthalpy values of 42.53 ± 0.09 and 36.27 ± 0.95 J/g, respectively. According to Siejak et al. (2025), higher enthalpy values may be indicative of increased thermal stability in lipid matrices.

These melting characteristics provide essential functional insights. The higher melting temperature of BD lipid suggests enhanced structural integrity, which may be advantageous in applications requiring solid or semi-solid lipid systems, such as spreads or emulsions. Conversely, the broad, low-temperature melting behavior of the PL lipid indicates high fluidity under ambient conditions, which may be beneficial for certain food applications, although its high PUFA content could predispose it to oxidative degradation. The GP lipid displayed intermediate properties, offering a balance of plasticity and flowability, potentially suitable for diverse food formulation scenarios. The DSC thermograms obtained in this study resemble those reported for other insect-derived oils, where multiple endothermic transitions indicate the heterogeneous TAG composition typical of insect lipids. Similar melting characteristics have been described for cricket, locust, and *Tenebrio molitor* oils, reinforcing the view that insect lipids possess complex crystalline structures influenced by diverse PUFA/MUFA ratios (Chantakun et al., 2024; Jeon et al., 2016; Martínez-Pineda et al., 2024).

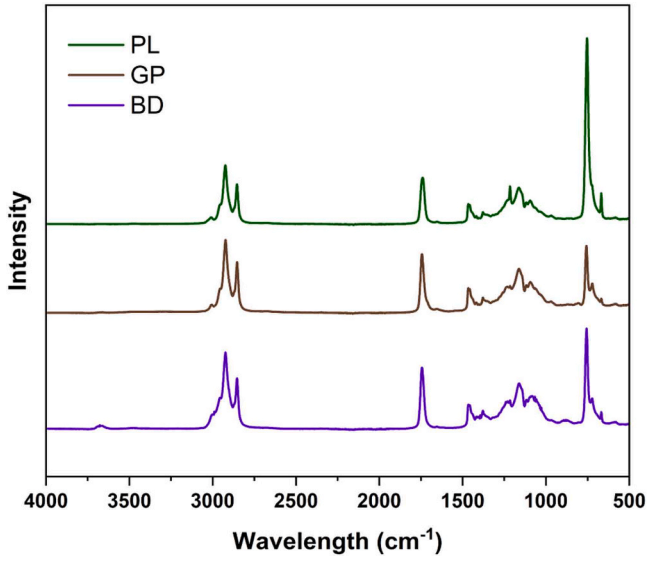

Fig. 5. The FTIR spectra of analyzed oils. GP - *Gromphadorhina portentosa*, PL - *Periplaneta lateralis*, BD - *Blaptica dubia*.

Table 6
Summary of FTIR absorption bands observed in lipid fractions of studied insect species.

Wavenumber (cm^{-1})	Vibrational mode	Chemical assignment	Sample relevance
~3009	=C-H stretching	*cis*-double bonds (PUFA)	Most intense in PL (highest PUFA content)
~2922	asymmetric CH_2 stretching	fatty acid chains	Strong in BD and GP (MUFA and SFA rich)
~2852	symmetric CH_2 stretching	fatty acid chains	Strong in BD and GP
~1743	C═O stretching	ester carbonyl in TAG	Present in all samples
~1465	CH_2 bending	fatty acid chains	Present in all samples
~1377	CH_3 bending	methyl groups	Present in all samples
1160–1235	C-O stretching	ester bonds in TAG	Present in all samples
~720	CH_2 rocking	long-chain SFA	Strongest in GP (highest SFA content)

3.8. FTIR spectroscopy

The FTIR spectra of lipid fractions isolated from GP, BD, and PL are presented in Fig. 5. All analyzed oils exhibited characteristic absorption bands corresponding to typical functional groups present in triacylglycerols (TAGs), allowing for differentiation among the samples based on their distinct fatty acid profiles. A detailed summary of the main absorption bands and their respective assignments is presented in Table 6. The strong absorption band at ~1743 cm^{-1}, present in all samples, is attributed to the stretching vibrations of ester carbonyl groups (C═O) in TAG molecules. The bands observed at ~2922 cm^{-1} and ~2852 cm^{-1} correspond to asymmetric and symmetric stretching vibrations of methylene (CH_2) groups, reflecting the length and degree of saturation of fatty acid chains. These bands were particularly intense in BD and GP samples, which contained higher proportions of monounsaturated (MUFA) and saturated fatty acids (SFA), respectively. The position of this band also confirms the highest PUFA share in the PL (3008 cm^{-1}) compared to the GP (3005 cm^{-1}). Another relevant band was observed near 720 cm^{-1}, attributed to CH_2 rocking vibrations, typically associated with long-chain saturated fatty acids. The most intense signal in this region was noted for GP oil, in agreement with its highest content of palmitic (19.01%) and stearic (6.06%) acids (Table 2). The well-developed spectra in the region of 1200 – 1000 cm^{-1} contain bands assigned to PO_2 groups (~1200 cm^{-1} and ~1090 cm^{-1}), indicate the presence of phospholipids in all the samples. The presence of bands, assigned to cholesterol can also be postulated – peaks at ~1470 cm^{-1} and ~1380 cm^{-1}. Based on the peak intensities, it can be assessed, that the content of this compound is the highest for GP and the lowest for PL samples, what strongly supports the findings reported in the 3.3 section. The observed FTIR profiles are in full agreement with the compositional data obtained from gas chromatography (fatty acid

Table 7
LF NMR relaxometry results (ms).

Sample	T_1	T_2
GP	110.84 ± 0.29^{c}	61.45 ± 1.90^{c}
BD	149.46 ± 0.47^{b}	74.95 ± 1.93^{b}
PL	262.33 ± 0.95^{a}	150.79 ± 1.97^{a}

Values marked with the same lowercase letter in columns do not differ significantly $^{p} > 0.05$. GP - *Gromphadorhina portentosa*, PL - *Periplaneta lateralis*, BD - *Blaptica dubia*.

profiles, see Section 3.1), DSC (melting behavior, see Section 3.6), and LF NMR (molecular dynamics, see Section 3.8) analyses.

Moreover, based on intensities of bands assigned to CH_2 and CH_3 groups (at ~2924 cm^{-1} and ~2954 cm^{-1}, respectively), and their ratio, a conclusion on average length and branching of fatty acids can be drawn (Stangierski et al., 2025). The higher the ratio is, the longer the aliphatic chains are present in the sample. On the other hand, the lower value of the ratio, accompanied by unchanged intensity of bands assigned to CH_2 groups, indicates high branching (each chain ends with a CH_3 group). For the insect oils studied, the intensities of bands assigned to CH_2 groups were similar for BD and GP, indicating a similar average length of chains. The ratios were: 2.43 for BD, 2.95 for GP, and 2.93 for PL, indicating that the average complexity of PL and GP oils is similar and noticeably higher than for BD oil.

3.9. LF NMR relaxometry

The molecular dynamics of oils were evaluated using low-field nuclear magnetic resonance (LF NMR) spectroscopy. Spin-lattice (T_1) and spin-spin (T_2) relaxation times are presented in Table 7 and provide insight into the molecular mobility and the physical state of the lipid matrix. The T_1 values, which reflect the recovery of longitudinal magnetization and are indicative of the overall molecular environment (Kimmich, 2024), varied significantly among the samples. PL oil exhibited the longest T_1 (>262 ms), suggesting the highest molecular mobility and lowest structural ordering. BD oil showed an intermediate T_1 value, while GP oil presented the shortest T_1, indicating more restricted proton mobility, possibly due to a higher content of saturated fatty acids and more ordered triacylglycerol packing (Kimmich, 2024; Resende et al., 2021).

A similar trend was observed for the T_2 relaxation times, which describe the decay of transverse magnetization and are influenced by molecular interactions and viscosity. PL oil again demonstrated the highest T_2 (>150 ms), followed by BD (~75 ms) and GP (~61 ms). Longer T_2 values are associated with less restricted molecular motion and lower intermolecular interactions (Baranowska, 2011; Baranowska & Rezler, 2015), which is consistent with the high PUFA content and low melting behavior of PL oil, as confirmed by DSC.

These results suggest that oils from different cockroach species exhibit distinct physical states at ambient temperature, governed by their fatty acid composition and molecular organization. The higher T_1 and T_2 values observed for PL indicate a more fluid and dynamic oil matrix, whereas the lower relaxation times in GP reflect increased structural rigidity, likely linked to its higher content of saturated lipids (Resende et al., 2021).

3.10. Characterization of Langmuir monolayers

During monolayer compression, depending on the interactions between molecules, the system can exist in different thermodynamic phases: liquid-expanded (LE), liquid (L), liquid-condensed (LC), and solid (S) (Kamińska et al., 2023). Surface pressure isotherms (π) as a function of the mean molecular area per oil molecule (A) were recorded during compression to obtain detailed information on how oil composition influences the thermodynamic state and phase transitions of the resulting oil monolayers (Fig. 6a). Based on the isotherm profiles, five key physicochemical parameters were calculated and interpreted to characterize the properties of these layers: the molecular area at the onset of π increase A_o, the molecular area at the point of monolayer collapse A_c, the collapse pressure π_c, the compressibility modulus C_s^{-1}, and the surface viscoelasticity modulus E. All measured values are presented in Table 8.

The recorded surface pressure π isotherms as a function of the molecular area A for the studied oils GP, BD, and PL exhibit a typical course characteristic of Langmuir-type monolayers. This indicates the ability of the lipid molecules present in the samples to form stable, insoluble monolayers at the air–water interface, which reflects their surface activity and sufficiently low solubility in the aqueous subphase. The A_o value serves as a significant indicator of the degree of molecular order during the initial stage of compression. Oils GP and PL show the highest values of this parameter 168.9 cm^2 and 168.2 cm^2, respectively, which

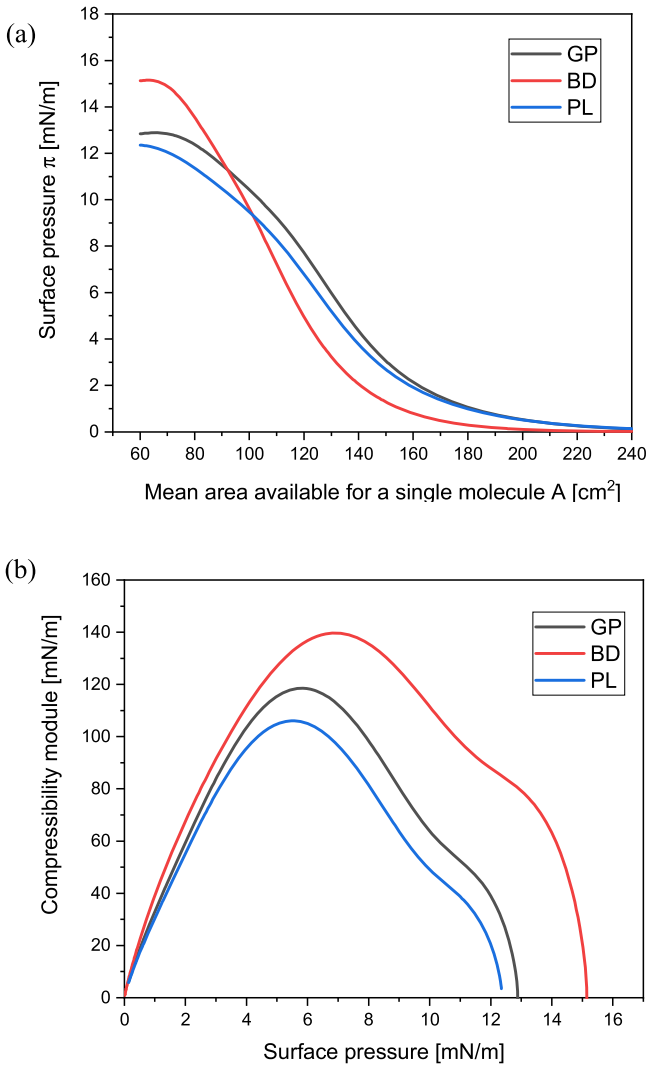

Fig. 6. π–A isotherms (a) and compression modulus versus surface pressure plots (b) for the Langmuir monolayers analyzed.

Table 8
The parameters designated from the isotherm profile.

Parameters π-A	GP	BD	PL
A_0 (cm^2)	168.9 ± 0.1^a	157.5 ± 0.1^c	168.2 ± 0.1^b
A_c (cm^2)	62.2 ± 0.1^a	60.9 ± 0.1^b	60.6 ± 0.1^c
π_c (mN/m)	12.9 ± 0.1^b	15.2 ± 0.1^a	12.3 ± 0.1^c
C_s^{-1} (mN/m)	118.9 ± 0.1^b	139.6 ± 0.1^a	106.5 ± 0.1^c
E (mN/m)	110.2 ± 0.1^b	131.5 ± 0.1^a	97.9 ± 0.1^c

The parameters designated from the isotherm profile: A_0—the average surface area available to the molecule, A_C—the average surface area available to the molecule at the collapse point, π_c—the surface pressure at the collapse point, C_s^{-1} — the compressibility modulus, and E — the surface viscoelasticity modulus. The data in the table are presented as the mean ± measurement uncertainty. Differences between results for respective oils marked with the same letter in the same row are statistically insignificant ($p < 0.05$). GP - *Gromphadorhina portentosa*, PL - *Periplaneta lateralis*, BD - *Blaptica dubia*.

implies that the molecules in these monolayers are initially less ordered, with greater intermolecular spacing. This phenomenon can be attributed to the presence of considerable amounts of PUFA, particularly linoleic acid (C18:2) and α-linolenic acid (C18:3), whose multiple double bonds cause kinks in the hydrocarbon chains and hinder their ability to pack linearly (Fidalgo Rodríguez et al., 2017; Hąc-Wydro & Wydro, 2007; Kamińska et al., 2025; Seoane et al., 2001; Tomoaia-Cotişel et al., 1987). In contrast, the BD oil, with an A_o of 157.5 cm^2, contains the highest content of oleic acid (C18:1 = 59.45%) and the lowest level of PUFA, which enables a more compact and ordered arrangement of molecules even at the early stages of compression.

The molecular area at the monolayer collapse point A_c also varies significantly between the oils, with the highest value observed for GP - 62.2 cm^2 and the lowest for PL −60.6 cm^2. Ac defines the threshold at which the layer can no longer maintain mechanical stability and collapses due to excessive molecular crowding. Lower A_c values may indicate either a higher degree of structural compactness or reduced resistance of the molecules to compression. In the case of PL, this effect can again be associated with the presence of PUFA, which reduce cohesion and monolayer integrity by disturbing the linear orientation of the molecules.

The collapse pressure π_c is a parameter expressing the maximum surface tension the monolayer can withstand before collapsing. BD exhibited the highest π_c value 15.2 mN/m, indicating the greatest monolayer stability. GP and PL oils had slightly lower values (12.9 and 12.3 mN/m, respectively), reflecting their lower mechanical resistance, which aligns with the hypothesis of a destabilizing effect of PUFA double bonds (Fidalgo Rodríguez et al., 2017; Hąc-Wydro & Wydro, 2007; Seoane et al., 2001; Tomoaia-Cotişel et al., 1987). This trend is confirmed in the literature, where an increasing degree of lipid unsaturation leads to weakened van der Waals interactions between molecules, resulting in lower π_c values and increased susceptibility to collapse (Davies & Rideal, 1963).

Based on the recorded π–A isotherms and measurements of monolayer behavior under dynamic conditions, the compressibility modulus C_s^{-1} and surface viscoelasticity E were determined. The analysis of these parameters offered additional insights into the mechanisms governing the stability of lipid monolayers and their physicochemical characteristics. The compressibility modulus C_s^{-1} , calculated from the derivative of the π–A isotherm, provides a quantitative measure of the layer's resistance to compression. The relationships between the compression modulus C_S^{-1} and surface pressure π (C_S^{-1} -π) presented in Fig. 6b allowed for a detailed analysis of the phase state of compressed Langmuir monolayers. According to the Davies and Rideal classification, C_s^{-1} values between 0 and 12.5 mN/m correspond to the gas phase, 12.5–50 mN/m to the liquid-expanded phase, 50–100 mN/m to the liquid-condensed phase, and 100–250 mN/m to the highly condensed liquid phase. Values above 250 mN/m indicate a solid phase (Davies & Rideal, 1963). All three oils demonstrated C_s^{-1} values within the 106.5–139.6 mN/m range, clearly indicating the highly condensed liquid phase. BD achieved the highest C_s^{-1} value (139.6 mN/m), confirming the high stiffness and resistance to deformation of its monolayer, attributed to the dominant presence of MUFA. GP (118.9 mN/m) and PL (106.5 mN/m) exhibited less compact structures and greater susceptibility to volume changes under external forces.

An additional parameter characterizing the elasticity of the monolayer under dynamic conditions is the surface viscoelasticity modulus E, which describes the monolayer's ability to resist deformation under oscillating barrier conditions. According to Vollhardt's classification, E values below 50 mN/m correspond to loose (dispersed) layers, values between 50 and 250 mN/m indicate elastic layers, and values above 250 mN/m signify rigid, highly compressed layers (Noskov & Bykov, 2018; Vollhardt, 1999). All three oils belong to the category of elastic layers (zone II), with BD exhibiting the highest E - 131.5 mN/m, confirming its superior resistance to dynamic disturbances. GP reached a value of 110.2 mN/m, and PL, with the lowest E of 97.9 mN/m, showed the weakest cohesion and least elasticity.

Based on these results, it can be clearly stated that the fatty acid profile of the studied oils plays a crucial role in determining their surface properties. BD, with the highest MUFA content (C18:1) and relatively low PUFA levels, forms the most compact, ordered, and compression-resistant monolayer. In contrast, PL, characterized by the highest PUFA content (C18:2 = 16.38%; C18:3 = 0.97%), forms a less ordered layer with lower stability and elasticity. GP occupies an intermediate position between these two extremes. These findings align with previous reports on the influence of hydrocarbon chain length and double bond number on the properties of Langmuir monolayers, confirming the key role of lipid chemical structure in monolayer organization and surface behavior (Kamińska et al., 2023, 2025; Noskov & Bykov, 2018; Siejak et al., 2025).

4. Limitations and future perspectives

This study provides an extensive multi-analytical characterization of cockroach-derived oils; however, several limitations must be acknowledged. First, although the physicochemical, molecular, and interfacial properties of the oils were comprehensively assessed, the present work remains exploratory and does not include toxicological analyses. Since cockroach species are not currently authorized as novel food ingredients within the European Union, further research must address safety aspects such as potential allergenicity, cytotoxicity, bioaccessibility, and the presence of any compounds of regulatory concern. Second, only a single extraction method (Folch) was applied, which ensures methodological consistency but may not fully represent how extraction conditions could influence lipid profiles, minor components, or oxidative behavior. Third, despite the use of advanced techniques including DSC, LF NMR, FTIR, and Langmuir monolayers to provide mechanistic insight into lipid molecular organization, the study did not evaluate functional performance in model food systems (e.g., emulsions, spreads, encapsulates). Future research should therefore integrate formulation studies to determine technological applicability. Additionally, environmental and dietary effects on lipid composition were not investigated; controlled feeding trials could clarify how rearing substrates modulate fatty acid profiles and antioxidant content. Finally, comprehensive risk assessment and compliance with Novel Food Regulation will be essential before considering any food-related applications. These steps will form the scientific foundation required to responsibly explore the potential of cockroach-derived lipids as sustainable alternative fat sources.

5. Conclusions

This study delivers a systematic, multi-analytical comparison of lipid fractions extracted from *Blaptica dubia*, *Gromphadorhina portentosa*, and *Periplaneta lateralis*, revealing pronounced interspecies differences in fatty acid composition, molecular organization, thermal behavior, and interfacial properties. The investigation was strictly exploratory and analytical in nature, and the results should not be interpreted as indicating suitability of these oils for human consumption or direct food application. Among the analyzed samples, *G. portentosa* oil demonstrated the highest physicochemical stability, which can be attributed to its more favorable SFA/MUFA/PUFA balance and significantly higher tocopherol content. These features were consistently reflected in the physicochemical analyses, including lower susceptibility to oxidative changes and more stable thermal and molecular behavior. *B. dubia* oil exhibited a well-balanced fatty acid profile and superior interfacial organization, forming the most compact and viscoelastic monolayers, indicative of a structurally coherent lipid system. In contrast, *P. lateralis* oil was characterized by a highly unsaturated fatty acid profile, elevated iodine value, and increased molecular mobility, which, while chemically distinctive, implies reduced intrinsic stability. Advanced analytical techniques such as FTIR, DSC, LF NMR, and Langmuir monolayer analysis proved effective in capturing subtle differences in lipid

structuring and dynamics, directly linked to compositional variability. The results underline the substantial chemical and physicochemical diversity of cockroach-derived lipids and provide a robust analytical foundation for future research focused on stabilization mechanisms, comparative lipid science, or regulatory-oriented risk assessment of insect-derived lipid fractions.

Funding acquisition

Not applicable.

Institutional Review Board Statement

Not applicable.

Informed Consent Statement

Not applicable.

Funding

This research received no external funding.

CRediT authorship contribution statement

Wiktoria Kamińska: Writing – original draft, Methodology, Investigation. **Aleksander Siger:** Investigation. **Anna Grygier:** Investigation. **Dominik Kmiecik:** Writing – review & editing, Investigation. **Jan Jakub Kucharski:** Writing – original draft, Investigation, Formal analysis, Data curation. **Ewa Ostrowska-Ligęza:** Writing – original draft, Methodology, Investigation. **Hanna Maria Baranowska:** Writing – review & editing, Writing – original draft, Methodology, Investigation. **Przemysław Łukasz Kowalczewski:** Writing – review & editing, Writing – original draft, Supervision, Resources, Methodology, Investigation, Funding acquisition, Formal analysis, Conceptualization. **Dominika Radzikowska-Kujawska:** Investigation, Conceptualization, Formal analysis, Methodology, Writing – original draft. **Krzysztof Dwiecki:** Investigation. **Przemysław Siejak:** Investigation.

Declaration of Generative AI and AI-assisted technologies in the writing process

During the preparation of this work, the authors used *ChatGPT (OpenAI)* solely for language editing purposes. After using this tool, the authors carefully reviewed and revised the content as necessary and take full responsibility for the final version of the manuscript.

Declaration of Competing Interest

The authors declare that they have no known competing financial interests or personal relationships that could have appeared to influence the work reported in this paper.

Data availability

Data will be made available on request.

References

AOCS, 2009a. Official Method Cd 1c-85. Calculated iodine value. Official Methods and Recommended Practices of the American Oil Chemists' Society (6th ed.). American Oil Chemists' Society, USA.

AOCS, 2009b. Official Method Ce 1h-05. Determination of cis-, trans-, saturated, monounsaturated and polyunsaturated fatty acids in vegetable or non-ruminant animal oils and fats by capillary GLC. Official methods and recommended practices of the american oil chemists' society. Reference 3, 1–29.

Baranowska, H.M., 2011. Water molecular properties in forcemeats and finely ground sausages containing plant fat. Food Biophys. 6 (1), 133–137. https://doi.org/10.1007/s11483-010-9190-z.

Baranowska, H.M., Rezler, R., 2015. Water binding analysis of fat-water emulsions. Food Sci. Biotechnol. 24 (6), 1921–1925. https://doi.org/10.1007/s10068-015-0253-2.

Barroso, F.G., De Haro, C., Sánchez-Muros, M.-J., Venegas, E., Martínez-Sánchez, A., Pérez-Bañón, C., 2014. The potential of various insect species for use as food for fish. Aquaculture 422–423, 193–201. https://doi.org/10.1016/j.aquaculture.2013.12.024.

Blomquist, G.J., Borgeson, C.E., Vundla, M., 1991. Polyunsaturated fatty acids and eicosanoids in insects. Insect Biochem. 21 (1), 99–106. https://doi.org/10.1016/0020-1790(91)90069-Q.

Budilarto, E.S., Kamal-Eldin, A., 2015. The supramolecular chemistry of lipid oxidation and antioxidation in bulk oils. Eur. J. Lipid Sci. Technol. 117 (8), 1095–1137. https://doi.org/10.1002/ejlt.201400200.

calder, P.C., 2015. Marine omega-3 fatty acids and inflammatory processes: effects, mechanisms and clinical relevance. Biochimica et Biophysica Acta (BBA) - Molecular Cell Biology Lipids 1851 (4), 469–484. https://doi.org/10.1016/j.bbalip.2014.08.010.

Carr, H.Y., Purcell, E.M., 1954. Effects of diffusion on free precession in nuclear magnetic resonance experiments. Phys. Rev. 94 (3), 630–638. https://doi.org/10.1103/PhysRev.94.630.

Chantakun, K., Petcharat, T., Wattanachant, S., Karim, M.S.B.A., Kaewthong, P., 2024. Fatty acid profile and thermal behavior of fat-rich edible insect oils compared to commonly consumed animal and plant oils. Food Sci. Anim. Resour. 44 (4), 790–804. https://doi.org/10.5851/kosfa.2024.e44.

Chen, J., Liu, H., 2020. Nutritional indices for assessing fatty acids: a mini-review. Int. J. Mol. Sci. 21 (16), 5695. https://doi.org/10.3390/ijms21165695.

Cichocki, W., Kmiecik, D., Baranowska, H.M., Staroszczyk, H., Sommer, A., Kowalczewski, P., 2023. Chemical characteristics and thermal oxidative stability of novel cold-pressed oil blends: GC, LF NMR, and DSC studies. Foods 12 (14), 2660. https://doi.org/10.3390/foods12142660.

Davies, J.T., Rideal, S.E.K., 1963. Interfacial phenomena. Academic Press.

Santos, Dos, Aguayo de Castro, J.V. De.A., Lima Cardoso, T.L., De Oliveira, C.A., De Minas, K.M.P., Oliveira, R.S., Talevi, S. de A., dos S, G., Pinheiro, M.N., Chang, M.R., Venancio, D.C.V., Da Silva, G.R., Kwiatkowski, A., 2025. Chemical composition of oils and fats from madagascar cockroach (*G. portentosa*), giant cockroach (*B. giganteus*), and mealworm (*T. molitor*). Orbit. Electron. J. Chem. 279–285. https://doi.org/10.17807/orbital.v16i4.22049.

Durrani, A.K., Khalid, M., Raza, A., Faiz Ul Rasool, I., Khalid, W., Akhtar, M.N., Ahmad Khan, A., Abdullah, Z., Khadijah, B., 2024. Clinical improvement, toxicity and future prospects of β-sitosterol: a review. CyTA - J. Food 22 (1). https://doi.org/10.1080/19476337.2024.2337886.

Eitenmiller, R.R., Lee, J., 2004. Vitamin E. CRC Press. https://doi.org/10.1201/9780203970140.

Fidalgo Rodríguez, J.L., Dynarowicz-Latka, P., Miñones Conde, J., 2017. Structure of unsaturated fatty acids in 2D system. Colloids Surf. B Biointerfaces 158, 634–642. https://doi.org/10.1016/j.colsurfb.2017.07.016.

Folch, J., Lees, M., Stanley, G.H.S., 1957. A simple method for the isolation and purification of total lipides from animal tissues. J. Biol. Chem. 226 (1), 497–509. https://doi.org/10.1016/S0021-9258(18)64849-5.

Gao, F., Birch, J., 2016. Oxidative stability, thermal decomposition, and oxidation onset prediction of carrot, flax, hemp, and canola seed oils in relation to oil composition and positional distribution of fatty acids. Eur. J. Lipid Sci. Technol. 118 (7), 1042–1052. https://doi.org/10.1002/ejlt.201500208.

Górska, A., Piasecka, I., Wirkowska-Wojdyła, M., Bryś, J., Kienc, K., Brzezińska, R., Ostrowska-Ligęza, E., 2023. Berry seeds—A by-product of the fruit industry as a source of oils with beneficial nutritional characteristics. Appl. Sci. 13 (8), 5114. https://doi.org/10.3390/app13085114.

Hąc-Wydro, K., Wydro, P., 2007. The influence of fatty acids on model cholesterol/phospholipid membranes. Chem. Phys. Lipids 150 (1), 66–81. https://doi.org/10.1016/j.chemphyslip.2007.06.213.

Hoshina, R., Endo, Y., Fujimoto, K., 2004. Effect of triacylglycerol structures on the thermal oxidative stability of edible oil. J. Am. Oil Chem. ' Soc. 81 (5), 461–465. https://doi.org/10.1007/s11746-004-0923-6.

Idris, Y.M.A., 2025. Lipids, fatty acids composition, and minor components of insects. Insect Oil as a Source of Nutraceuticals. Elsevier, pp. 127–149. https://doi.org/10.1016/B978-0-443-23934-2.00008-1.

Iqbal, B., Alabbosh, K.F., Jalal, A., Suboktagin, S., Elboughdiri, N., 2025. Sustainable food systems transformation in the face of climate change: strategies, challenges, and policy implications. Food Sci. Biotechnol. 34 (4), 871–883. https://doi.org/10.1007/s10068-024-01712-y.

ISO, 2008. ISO 8534:2008 animal and vegetable fats and oils. determination of water content - Karl Fischer method. International Organization for Standardization.

Jeon, Y.-H., Son, Y.-J., Kim, S.-H., Yun, E.-Y., Kang, H.-J., Hwang, I.-K., 2016. Physicochemical properties and oxidative stabilities of mealworm (Tenebrio molitor) oils under different roasting conditions. Food Sci. Biotechnol. 25 (1), 105–110. https://doi.org/10.1007/s10068-016-0015-9.

Jing, X., Behmer, S.T., 2020. Insect sterol nutrition: physiological mechanisms, ecology, and applications. Annu. Rev. Entomol. 65 (1), 251–271. https://doi.org/10.1146/annurev-ento-011019-025017.

Kamal-Eldin, A., 2006. Effect of fatty acids and tocopherols on the oxidative stability of vegetable oils. Eur. J. Lipid Sci. Technol. 108 (12), 1051–1061. https://doi.org/10.1002/ejlt.200600090.

Kamińska, W., Cichocki, W., Baranowska, H.M., Walkowiak, K., Kmiecik, D., Kowalczewski, P., 2023. Characteristics of Langmuir monomolecular monolayers

formed by the novel oil blends. Open Chem. 21 (1), 20230173. https://doi.org/10.1515/chem-2023-0173.
Kamińska, W., Rzyska-Szczupak, K., Przybylska-Balcerek, A., Stuper-Szablewska, K., Dembska, A., Neunert, G., 2025. Behavior at air/water interface and oxidative stability of vegetable oils analyzed through langmuir monolayer technique. Molecules 30 (1), 170. https://doi.org/10.3390/molecules30010170.
Kapoor, B., Kapoor, D., Gautam, S., Singh, R., Bhardwaj, S., 2021. Dietary polyunsaturated fatty acids (PUFAs): uses and potential health benefits. Curr. Nutr. Rep. 10 (3), 232–242. https://doi.org/10.1007/s13668-021-00363-3.
Khalili Tilami, S., Kouřimská, L., 2022. Assessment of the nutritional quality of plant lipids using atherogenicity and thrombogenicity indices. Nutrients 14 (18), 3795. https://doi.org/10.3390/nu14183795.
Kimmich, R., 2024. Nuclear magnetic relaxation and molecular dynamics. Royal Society of Chemistry. https://doi.org/10.1039/9781837671915.
Kmiecik, D., Fedko, M., Siger, A., Kowalczewski, P.Ł., 2022. Nutritional quality and oxidative stability during thermal processing of cold-pressed oil blends with 5:1 ratio of ω6/ω3 fatty acids. Foods 11 (8), 1081. https://doi.org/10.3390/foods11081081.
Kolobe, S.D., Manyelo, T.G., Malematja, E., Sebola, N.A., Mabelebele, M., 2023. Fats and major fatty acids present in edible insects utilised as food and livestock feed. Vet. Anim. Sci. 22, 100312. https://doi.org/10.1016/j.vas.2023.100312.
Lehmad, M., Lhomme, P., El Hachimi, Y., Abdenouri, N., 2026. Advances in processing techniques and sustainable valorization of black soldier fly (Hermetia illucens) larvae: a comprehensive review. Eur. Food Res. Technol. 252 (3), 109. https://doi.org/10.1007/s00217-026-05050-7.
Luviano, A.S., Campos-Terán, J., Langevin, D., Castillo, R., Espinosa, G., 2019. Mechanical properties of DPPC–POPE mixed langmuir monolayers. Langmuir 35 (51), 16734–16744. https://doi.org/10.1021/acs.langmuir.9b02995.
Martínez-Pineda, M., Juan, T., Antoniewska-Krzeska, A., Vercet, A., Abenoza, M., Yagüe-Ruiz, C., Rutkowska, J., 2024. Exploring the potential of yellow mealworm (tenebrio molitor) oil as a nutraceutical ingredient. Foods 13 (23), 3867. https://doi.org/10.3390/foods13233867.
Martín-Torres, S., Tello-Jiménez, J.A., López-Blanco, R., González-Casado, A., Cuadros-Rodríguez, L., 2022. Monitoring the shelf life of refined vegetable oils under market storage conditions—a kinetic chemofoodmetric approach. Molecules 27 (19), 6508. https://doi.org/10.3390/molecules27196508.
Meiboom, S., Gill, D., 1958. Modified spin-echo method for measuring nuclear relaxation times. Rev. Sci. Instrum. 29 (8), 688–691. https://doi.org/10.1063/1.1716296.
Mishra, S.K., Belur, P.D., Iyyaswami, R., 2021. Use of antioxidants for enhancing oxidative stability of bulk edible oils: a review. Int. J. Food Sci. & Technol. 56 (1), 1–12. https://doi.org/10.1111/ijfs.14716.
Moruzzo, R., Mancini, S., Guidi, A., 2021. Edible insects and sustainable development goals. Insects 12 (6), 557. https://doi.org/10.3390/insects12060557.
Mudalungu, C.M., Mokaya, H.O., Tanga, C.M., 2023a. Beneficial sterols in selected edible insects and their associated antibacterial activities. Sci. Rep. 13 (1), 10786. https://doi.org/10.1038/s41598-023-37905-4.
Mudalungu, C.M., Mokaya, H.O., Tanga, C.M., 2023b. Beneficial sterols in selected edible insects and their associated antibacterial activities. Sci. Rep. 13 (1), 10786. https://doi.org/10.1038/s41598-023-37905-4.
Nogueira, M.S., Scolaro, B., Milne, G.L., Castro, I.A., 2019. Oxidation products from omega-3 and omega-6 fatty acids during a simulated shelf life of edible oils. LWT 101, 113–122. https://doi.org/10.1016/j.lwt.2018.11.044.
Noskov, B.A., Bykov, A.G., 2018. Dilational rheology of monolayers of nano- and micropaticles at the liquid-fluid interfaces. Curr. Opin. Colloid & Interface Sci. 37, 1–12. https://doi.org/10.1016/j.cocis.2018.05.001.
Oh, S., Yi, B.R., Park, J.W., Kim, M.-J., Lee, J.H., 2015. Effects of relative humidity and neutral emulsifier on oxidative stability of corn oil during room temperature storage. J. Korean Soc. Appl. Biol. Chem. 58 (4), 521–526. https://doi.org/10.1007/s13765-015-0073-3.
Palupi, E., Nasir, S.Q., Jayanegara, A., Susanto, I., Ismail, A., Iwansyah, A.C., Setiawan, B., Sulaeman, A., Damanik, M.R.M., Filianty, F., 2025. Meta-analysis on the fatty acid composition of edible insects as a sustainable food and feed. Future Foods 11, 100529. https://doi.org/10.1016/j.fufo.2024.100529.
Perez-Santaescolastica, C., De Pril, I., Van De Voorde, I., Fraeye, I., 2023. Fatty acid and amino acid profiles of seven edible insects: focus on lipid class composition and protein conversion factors. Foods 12 (22), 4090. https://doi.org/10.3390/foods12224090.
Petersen, K.S., Maki, K.C., Calder, P.C., Belury, M.A., Messina, M., Kirkpatrick, C.F., Harris, W.S., 2024. Perspective on the health effects of unsaturated fatty acids and commonly consumed plant oils high in unsaturated fat. Br. J. Nutr. 132 (8), 1039–1050. https://doi.org/10.1017/S0007114524002459.
Piotrowska-Kirschling, A., Drzeżdżon, J., Chmurzyński, L., Jacewicz, D., 2018. Critical micellar concentration and methods of its determination (in Polish). Wiadomości Chem. 72, 815–828.
Resende, M.T., Osheter, T., Linder, C., Wiesman, Z., 2021. Proton low field NMR relaxation time domain sensor for monitoring of oxidation stability of PUFA-rich oils and emulsion products. Foods 10 (6), 1385. https://doi.org/10.3390/foods10061385.
Rudzińska, M., Cieślik-Boczula, K., Grygier, A., Kmiecik, D., Dwiecki, K., Jarzębski, M., 2025. Stigmasterol and its esters encapsulated in liposomes: characterization, stability, and derivative formation. Food Chem. 465, 142039. https://doi.org/10.1016/j.foodchem.2024.142039.
Rumpold, B.A., Schlüter, O.K., 2013. Potential and challenges of insects as an innovative source for food and feed production. Innov. Food Sci. & Emerg. Technol. 17, 1–11. https://doi.org/10.1016/j.ifset.2012.11.005.
Sabolová, M., Adámková, A., Kouřimská, L., Chrpová, D., Pánek, J., 2016. Minor lipophilic compounds in edible insects. Potravina Slovak J. Food Sci. 10 (1), 400–406. https://doi.org/10.5219/605.
Seoane, R., Dynarowicz-Tstka, P., Miñones Jr, J., Rey-Gómez-Serranillos, I., 2001. Mixed Langmuir monolayers of cholesterol and `essential' fatty acids. Colloid & Polym. Sci. 279 (6), 562–570. https://doi.org/10.1007/s003960000453.
Sharma, S.K., Barthwal, R., Saini, D., Rawat, N., 2022. Chemistry of food fats, oils, and other lipids. Advances in Food Chemistry. Springer Nature Singapore, pp. 209–254. https://doi.org/10.1007/978-981-19-4796-4_6.
Shelomi, M., 2015. Why we still don't eat insects: assessing entomophagy promotion through a diffusion of innovations framework. Trends Food Sci. & Technol. 45 (2), 311–318. https://doi.org/10.1016/j.tifs.2015.06.008.
Siddiqui, S.A., Hadus, M.C.I., Fitriani, A., Guleria, V., Kuppusamy, S., Bhattacharjee, B., Yudhistira, B., Maggiolino, A., 2024. Edible cockroaches as food and feed – A systematic review on health benefits, nutritional aspects and consumer acceptance. J. Insects Food Feed 1–43. https://doi.org/10.1163/23524588-00001138.
Siejak, P., Neunert, G., Kamińska, W., Dembska, A., Polewski, K., Siger, A., Grygier, A., Tomaszewska-Gras, J., 2025. A crude, cold-pressed oil from elderberry (*Sambucus nigra* L.) seeds: comprehensive approach to properties and characterization using HPLC, DSC, and multispectroscopic methods. Food Chem. 464, 141758. https://doi.org/10.1016/j.foodchem.2024.141758.
Siger, A., Kachlicki, P., Czubiński, J., Polcyn, D., Dwiecki, K., Nogala-Kalucka, M., 2014. Isolation and purification of plastochromanol-8 for HPLC quantitative determinations. Eur. J. Lipid Sci. Technol. 116 (4), 413–422. https://doi.org/10.1002/ejlt.201300297.
Siger, A., Michalak, M., 2016. The long-term storage of cold-pressed oil from roasted rapeseed: effects on antioxidant activity and levels of canolol and tocopherols. Eur. J. Lipid Sci. Technol. 118 (7), 1030–1041. https://doi.org/10.1002/ejlt.201500183.
Simopoulos, A.P., 2002. Omega-3 fatty acids in inflammation and autoimmune diseases. J. Am. Coll. Nutr. 21 (6), 495–505. https://doi.org/10.1080/07315724.2002.10719248.
Stangierski, J., Rezler, R., Siejak, P., Walkowiak, K., Masewicz, Ł., Kawecki, K., Baranowska, H.M., 2025. An instrumental analysis of changes in the physicochemical and mechanical properties of smoked and mould salamis during storage. J. Food Eng. 392, 112486. https://doi.org/10.1016/j.jfoodeng.2025.112486.
Tomoaia-Cotişel, M., Zsakó, J., Mocanu, A., Lupea, M., Chifu, E., 1987. Insoluble mixed monolayers. J. Colloid Interface Sci. 117 (2), 464–476. https://doi.org/10.1016/0021-9797(87)90407-3.
Tzompa-Sosa, D.A., Yi, L., Van Valenberg, H.J.F., Van Boekel, M.A.J.S., Lakemond, C.M. M., 2014. Insect lipid profile: aqueous versus organic solvent-based extraction methods. Food Res. Int. 62, 1087–1094. https://doi.org/10.1016/j.foodres.2014.05.052.
Ulbricht, T.L.V., Southgate, D.A.T., 1991. Coronary heart disease: seven dietary factors. Lancet 338 (8773), 985–992. https://doi.org/10.1016/0140-6736(91)91846-M.
Van Huis, A., 2013. Potential of insects as food and feed in assuring food security. Annu. Rev. Entomol. 58 (1), 563–583. https://doi.org/10.1146/annurev-ento-120811-153704.
Van Huis, A., 2020. Nutrition and health of edible insects. Curr. Opin. Clin. Nutr. & Metab. Care 23 (3), 228–231. https://doi.org/10.1097/MCO.0000000000000641.
Van Huis, A., 2022. Edible insects: challenges and prospects. Èntomol. Res. 52 (4), 161–177. https://doi.org/10.1111/1748-5967.12582.
Vollhardt, D., 1999. Phase transition in adsorption layers at the air–water interface. Adv. Colloid Interface Sci. 79 (1), 19–57. https://doi.org/10.1016/S0001-8686(98)00073-6.
Węglarz, W.P., Harańczyk, H., 2000. Two-dimensional analysis of the nuclear relaxation function in the time domain: the program CracSpin. J. Phys. D Appl. Phys. 33 (15), 1909–1920. https://doi.org/10.1088/0022-3727/33/15/322.
Wijerathna-Yapa, A., Pathirana, R., 2022. Sustainable agro-food systems for addressing climate change and food security. Agriculture 12 (10), 1554. https://doi.org/10.3390/agriculture12101554.
Wirkowska, M., Ostrowska-Ligęza, E., Górska, A., Koczoń, P., 2012. Thermal properties of fats extracted from powdered baby formulas. J. Therm. Anal. Calorim. 110 (1), 137–143. https://doi.org/10.1007/s10973-012-2245-2.
Wirkowska-Wojdyła, M., Ostrowska-Ligęza, E., Górska, A., Bryś, J., 2022. Application of chromatographic and thermal methods to study fatty acids composition and positional distribution, oxidation kinetic parameters and melting profile as important factors characterizing amaranth and quinoa oils. Appl. Sci. 12 (4), 2166. https://doi.org/10.3390/app12042166.
Yap, J.W.-L., Lee, Y.-Y., Tang, T.-K., Chong, L.-C., Kuan, C.-H., Lai, O.-M., Phuah, E.-T., 2023. Fatty acid profile, minor bioactive constituents and physicochemical properties of insect-based oils: a comprehensive review. Crit. Rev. Food Sci. Nutr. 63 (21), 5231–5246. https://doi.org/10.1080/10408398.2021.2015681.
Ying, Q., Wojciechowska, P., Siger, A., Kaczmarek, A., Rudzińska, M., 2018. Phytochemical content, oxidative stability, and nutritional properties of unconventional cold-pressed edible oils. J. Food Nutr. Res. 6 (7), 476–485. https://doi.org/10.12691/jfnr-6-7-9.